Molecular Biology of the Cell
Vol. 16, 4485–4494, October 2005

Induction of Cytokinesis Is Independent of Precisely Regulated Microtubule Dynamics[V]

Laila I. Strickland, Erin J. Donnelly, and David R. Burgess

Boston College, Chestnut Hill, MA 02467

Submitted April 12, 2005; Revised June 28, 2005; Accepted July 6, 2005
Monitoring Editor: Ted Salmon

Astral microtubules (MTs) emanating from the mitotic apparatus (MA) during anaphase are required for stimulation of cytokinesis in eggs. We have used green fluorescent protein-labeled EB1 to observe MT dynamics during mitosis and cytokinesis in normal sea urchin eggs. Analysis of astral MT growth rates during anaphase shows that MTs contact the polar cortex earlier than the equatorial cortex after anaphase onset but that a normal cleavage furrow is not induced until contact with MTs has been achieved throughout the cortex. To assess the role of MT dynamics in initiation of cytokinesis, we used a collection of small molecule drugs to affect dynamics. Hexylene glycol resulted in rapid astral elongation due to decreased MT catastrophe and precocious furrowing. Taxol suppressed MT dynamics but did not inhibit furrow induction when the MA was manipulated toward the cortex. Urethane resulted in short, highly dynamic astral MTs with increased catastrophe that also stimulated furrowing upon being brought into proximity to the cortex. Our findings indicate that astral MT contact with the cortex is necessary for furrow initiation but that the dynamic state of astral MTs does not affect their competency to stimulate furrowing.

INTRODUCTION

Cytokinesis is the process by which the cytoplasm is divided at the end of mitosis to form two daughter cells. Much has been learned about the actomyosin ring that generates the contractile force required for cytokinesis; however, many questions remain regarding mechanisms that specify the place and time for contractile ring assembly and activation. The cleavage furrow normally bisects the mitotic apparatus (MA) at the plane of the former metaphase plate (Wilson, 1928), and microtubules (MTs) of the MA are essential for communication of the contractile signals (Beams and Evans, 1940). Several models have been proposed to describe the initiation of cytokinesis, each of which attributes the source of the signal to a different MT population within the MA (Balasubramanian *et al*., 2004; Burgess and Chang, 2005). In one of the most well studied cell types, the cleaving echinoderm egg, positioning of the furrow is determined by equatorial stimulation from two asters and not by the bundled MTs of the spindle midzone, kinetochores, or by the polar astral MTs (Rappaport, 1996), which may play a stimulatory role in other cell types (Burgess and Chang, 2005; D'Avino *et al*., 2005; Glotzer, 2005). However, the nature, degree, and extent of contact between the astral MTs and the cortex required for stimulation of cytokinesis is not yet determined.

Changes in MT dynamics facilitate structural reorganization of the MA during cell division. At the metaphase–anaphase transition astral MTs elongate due to decreased catastrophe or increased rescue, kinetochore MTs shorten to segregate the chromosomes, and spindle midzone MTs grow to promote separation of the spindle poles (DeBrabander *et al*., 1986; Snyder and Mullins, 1993; Zhai *et al*., 1995; Mallavarapu *et al*., 1999; Rusan *et al*., 2002; Piehl *et al*., 2004). Anaphase onset is a necessary condition for stimulation of cytokinesis in cleaving eggs (Shuster and Burgess, 2002), and it is at this time that astral MTs undergo a dramatic elongation toward the cortex. Changes in MT dynamics are essential for induction of cytokinesis due to the necessity of astral MTs to grow at anaphase onset to contact the cell cortex. However, the nature of MTs competent to induce furrowing remains unclear.

One hypothesis for furrow formation is that the cortex is sensitive to or alters the dynamic state of MTs upon MT contact with the cell cortex. A recent report suggested that MT stabilization is required for stimulation of cytokinesis because furrowing correlated with sites of contact between chromosome-associated stable MTs and the cortex and that selective stabilization of equatorially directed astral or peripheral spindle MTs occurs as a result of their elongation past the chromosomes during anaphase in mammalian tissue cells (Canman *et al*., 2003). Astral MTs not associated with chromosomes that contacted the cortex but then retracted due to catastrophe were not observed to correlate with furrow ingression (Canman *et al*., 2003). On the other hand, there are conflicting reports on the ability of taxol-stabilized astral MTs to induce furrowing (Salmon and Wolniak, 1984; Hamaguchi, 1998). Although these reports suggest that some period of sustained contact with the cortex is required for furrow stimulation, they do not resolve the question of whether the stabilized dynamic state of these astral MTs participates in positioning and signaling cytokinesis.

We describe here a complete analysis of the geometry of the MA relative to the cortex in dividing eggs. We have performed a series of experiments designed to characterize MT dynamics in dividing sea urchin eggs by using confocal time-lapse imaging of live cells injected with green fluorescent protein (GFP)-EB1 as it tracks the plus ends of elongat-

This article was published online ahead of print in *MBC in Press* (http://www.molbiolcell.org/cgi/doi/10.1091/mbc.E05–04–0305) on July 12, 2005.

[V] The online version of this article contains supplemental material at *MBC Online* (http://www.molbiolcell.org).

Address correspondence to: David R. Burgess (david.burgess@bc.edu).

ing microtubules and then test whether the dynamic state of microtubules is important for initiation of cytokinesis. A battery of small molecule compounds that modulate MT dynamics was applied to cleavage stage sea urchin embryos, and then the ability of the MA to stimulate furrowing was assessed. Our results indicate that furrow initiation occurs after contact between the cortex and astral MTs has been achieved and that the dynamic state of MTs before cortical contact is not relevant to their ability to stimulate cytokinesis.

MATERIALS AND METHODS

Collection and Fertilization of Sea Urchin Eggs

Gametes were collected from *Lytechinus pictus* by intracoelemic injection of 0.5 M KCl. Jelly coats were dissolved from eggs in calcium-free sea water (CaFSW) before fertilization. Sperm were diluted 1000× in sea water and acrosome activated by vigorous aeration. They were then added dropwise to eggs in sea water until fertilization was achieved. Fertilization envelopes were removed 1 min after fertilization by pouring eggs in CaFSW through Nitex mesh.

Chemical Modification of Microtubule Dynamics

Microtubule dynamics of mitotic cells in early cleavage stage embryos were modulated by treatment with either 50 mM urethane, 0.75% hexylene glycol, 0.01 μM nocodazole, or 100 μM taxol. Taxol was microinjected into cells at discrete times and locations. Conditions for microinjection and micromanipulation are as described previously (Shuster and Burgess, 1999). All other treatments were applied after nuclear envelope breakdown, but before anaphase onset.

Fixation and Immunofluorescence

L. pictus embryos were cultured to the desired stage in CaFSW, washed once in a 10× volume of isolation buffer (80 mM PIPES, 1 M glycerol, 5 mM EGTA, 5 mM $MgCl_2$), and then incubated on an end-over-end rotator at room temperature for 1–3 h in a 10× volume fixation buffer (80 mM PIPES, 1 M glycerol, 5 mM EGTA, 5 mM $MgCl_2$, 3.7% formaldehyde, 0.5% NP-40 (Strickland *et al*., 2004). After fixation, embryos were washed three times in 10× volumes of phosphate-buffered saline (PBS) and subsequently stained for immunofluorescence. Immunofluorescence was performed by incubating the embryos on an end-over-end rotator with the appropriate dilution of primary antibody or secondary antibody in PBS with 3% bovine serum albumin for 1–3 h at room temperature. Three washes in a 10× volume of PBS were performed after each incubation.

Antibodies

E7 mouse anti-tubulin was obtained from Developmental Studies Hybridoma Bank (University of Iowa, Iowa City, IA) and used for immunofluorescence at a dilution of 1:50. Alexa488-anti-mouse was obtained from Molecular Probes (Eugene, OR) and used for secondary detection of immunofluorescence at a dilution of 1:200.

Expression, Purification, and Microinjection of GFP-EB1

A pGEX plasmid containing His-tagged hEB1-EGFP was obtained from Lynne Cassimeris (Piehl and Cassimeris, 2003) and transformed into the BL21-D3pLys strain of *Escherichia coli*. Then, 200 mM isopropyl β-D-thiogalactoside was used to induce expression, and the fusion protein was purified on a NiNT3 column. Purified protein was then dialyzed into injection buffer (150 mM aspartic acid, pH 7.2, 10 mM HEPES) and stored at −80°C until use. Protein was injected at a concentration of 1 mg/ml as described previously (Shuster and Burgess, 1999).

Image Acquisition and Fluorescence Quantitation

Wide field fluorescence microscopy and Nomarski differential interference contrast (DIC) were performed on a Nikon TE200. Chromosome movements during mitosis and cytokinesis were visualized with Hoechst stain, diluted 1:10,000 (Molecular Probes). Confocal images were acquired on a Leica TCS SP2 microscope equipped with an argon/krypton laser.

Quantitation of microtubule density was based on fluorescence intensity of confocal immunofluorescent images using the Leica software. Briefly, a rectangular region of interest (ROI) was selected at the polar region of an image and then copied to the equatorial region. The quantitation function was applied to determine the fluorescence intensity based on pixel density of each ROI. To account for differences in raw fluorescence values between one image and the next, the polar intensity value was divided by the equatorial intensity value, generating a ratio of fluorescence at the pole relative to fluorescence at the equator for each image. The average ratio was then calculated for each group of images analyzed.

Determination of MT Growth Rates

Microtubule growth rates were measured in anaphase-stage cells that had been microinjected with hEB1-EGFP by time-lapse confocal microscopy. To track the plus ends of individual microtubules, we zoomed into one quadrant of the cell that represented polar and equatorial astral microtubule growth. Microtubules whose trajectory of growth remained within the confocal plane for a minimum of 15 s were measured. Each acquisition required a 4.5-s scan time, and images were acquired every 5 s. Therefore, at least three time-lapse frames of the same microtubule were required for each grow rate measurement. Measurements from each frame were made from the center of the hEB1-EGFP tip to the site of nucleation at the centrosome, and the measured distance over time represents the rate of elongation. Two polar and equatorial astral MT growth rates were obtained from the same cell, and the measurements were repeated in three different cells.

RESULTS

Microtubules Undergo a Dramatic Change in Their Dynamic Properties at the Metaphase–Anaphase Transition

The distribution of microtubules in fertilized sea urchin eggs as they undergo division reflects their dynamic changes at anaphase onset. Wide field fluorescent microscopy of fixed embryos stained with antibodies against tubulin reveals that the egg is virtually full of MTs at the time of cleavage stimulus (Figure 1A). When viewed by confocal microscopy, specific structural characteristics of the MA can be seen (Figure 1B). At metaphase, which lasts only 5 min in this cell, the asters have an average diameter of 30 μm and the spindle averages 29.8 μm in pole-to-pole length (Figure 1 and Table 1). We determined the distances between the asters and the cell cortex at both the poles and equatorial surfaces from confocal images of MT immunofluorescence in metaphase cells (Figure 2 and Table 1). Measurements were made from the periphery of the astral MTs to the edge of the cell. These measurements represent the distances that the asters must expand beyond their metaphase diameter to contact the cortex after anaphase onset. At metaphase, distance from the astral periphery to the polar cortex is 17.7 μm, and the distance from the astral periphery to the equatorial cortex is 34.3 μm. During anaphase, the asters expand until the tips of the MTs contact the cortex. The bundled MTs of the spindle midzone or central spindle do not occur until after furrow initiation has taken place (Figure 1B)

If astral MT elongation at anaphase occurs at a uniform rate in all directions, then the MTs emanating toward the poles should be the first to contact the cell cortex. To visualize MT growth, we microinjected GFP-EB1 into fertilized eggs and observed live MT dynamics by time-lapse confocal microscopy (Figure 1C and Supplemental Movies 1–5). GFP-EB1 localized prominently to the centrosomes and spindle midzone and also decorated the tips of astral MTs that rapidly alternated between periods of growth and catastrophe during metaphase, and abruptly began to elongate at anaphase onset, reflecting a decrease of MT catastrophe (see below). Kinetochore MTs shortened, the centrosomes expanded to form elliptical structures, and the spindle midzone MTs became bundled after initiation of anaphase. Microinjection of GFP-EB1 did not affect mitotic progression, morphology of the MA, rate of chromosome movement, timing of cytokinesis relative to anaphase onset, or duration of furrow ingression (our unpublished data).

High-magnification views of specific populations of MTs allowed us to track the growth of individual MTs through several 5-s acquisition periods (Figure 1D). We compared the growth rates of astral anaphase MTs directed toward the poles with those of astral anaphase MTs directed toward the equatorial cortex, and found that populations of astral MTs

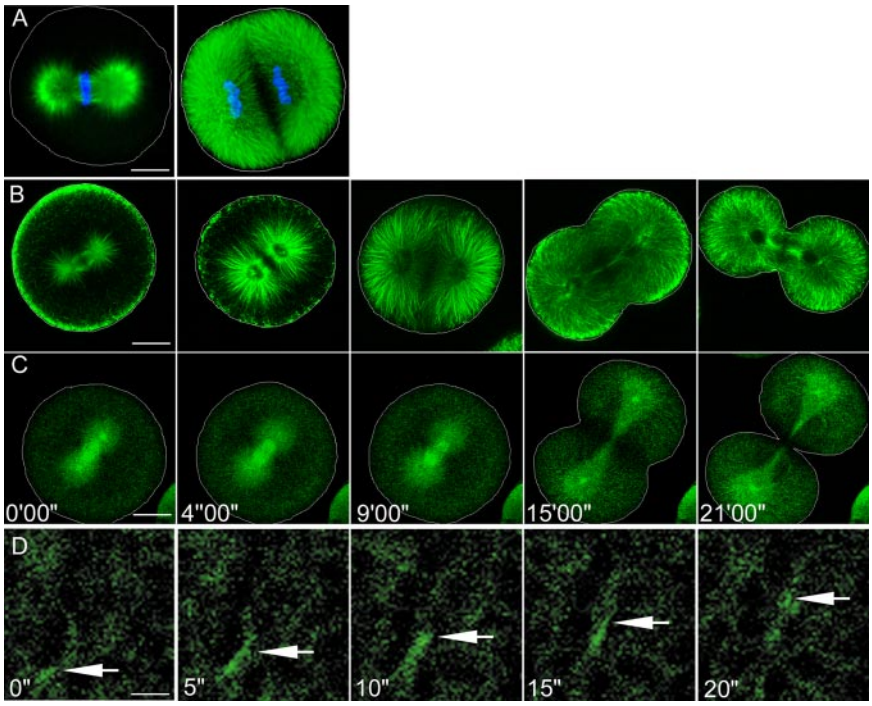

Figure 1. Structure and dynamics of microtubules of the mitotic apparatus during completion of mitosis and cytokinesis. Cell outlines are shown in white when necessary. (A) Wide field fluorescence microscopy of microtubules (green) stained by immunofluorescence and chromosomes DNA (blue) during metaphase and anaphase in a dividing sea urchin egg. After the metaphase-anaphase transitions, the asters expand substantially, filling the egg with microtubules. Bar, 25 μm. (B) Confocal imaging of fixed eggs at different stages of mitotic progression and cytokinesis, stained for microtubules by immunofluorescence. After anaphase onset, the centrosomes expand and the astral microtubules elongate, contacting the polar cortex first, and then establishing contact at the equator before furrow ingression. Bar, 25 μm. (C) Confocal time-lapse of a GFP-EB1-microinjected egg as it proceeds through mitosis and cytokinesis. GFP-EB1 decorates the plus ends of elongating MTs and localizes abundantly to the spindle structures. Abrupt expansion of the asters is observed after anaphase onset, before furrow ingression. Bar, 25 μm. (D) Confocal time-lapse of a GFP-EB1 injected egg showing elongation of an astral microtubule during anaphase. The decoration of the MT plus ends by GFP-EB1 formed comet tails that were used to measure MT growth rates relative to their site of nucleation at the centrosome. Bar, 5 μm.

elongate at similar rates of 10 ± 2 and 8.2 ± 2 μm/min, respectively (Table 2). Because astral MTs elongate at a comparable rate in all directions at anaphase onset, yet the distance to the equator is nearly twice the distance to the pole, we predict that the polar-directed MTs contact the cortex 2–3 min after anaphase onset, and equatorially directed MTs contact the cortex 3–5 min after anaphase onset. These estimations of time of contact are consistent with our observations of GFP-EB1 time-lapse movies in which the whole cell is in the field of view and the polar and equatorial astral MT populations can be observed during anaphase progression. When we monitored mitotic progression by staining the chromosomes with Hoechst, we found that cytokinesis begins an average of 13 min after anaphase onset (Table 2). Therefore, MTs reach all parts of the cortex 7–10 min before furrow ingression.

The polar relaxation hypothesis of furrow initiation suggests that due to a local concentration of astral influence at the poles, relative to the equator, cortical tension in the poles is decreased and therefore furrows form at the equator (Wolpert, 1960; White and Borisy, 1983; Dechant and Glotzer, 2003). Meanwhile, the equatorial stimulation hypothesis proposes that a maximum of stimulatory signals arise at the equator due to the overlapping influence from both asters in this region (Rappaport, 1996). Both of these classical models assume that a differential of MT density in the cortex at the time of stimulation, and not the biochemical character of the MT plus ends, is sufficient to account for furrow ingression (Dechant and Glotzer, 2003). Polar relaxation requires a density minimum at the equator, and equatorial stimulation requires a density maximum at the equator. To address this conflict in sea urchin eggs, we measured MT density in different regions of the cortex based on fluorescence intensity from confocal images of eggs stained for tubulin (Figure 3A). We defined polar and equatorial regions of interest for eggs that had just undergone anaphase onset, but had not yet begun to elongate in preparation for division (early), eggs in later anaphase at the time of furrow induction that were oval-shaped due to anaphase B spindle pole separation (mid), and eggs that have just begun to

Table 1. Geometric parameters of dividing *L. pictus* eggs

Measurement	Control	HG	Taxol	Urethane
Cell diameter (μm)	108 ± 4	108 ± 4	108 ± 4	108 ± 4
Metaphase spindle length (μm)	29.8 ± 3	35.4 ± 4	21.8 ± 0.5	19.7 ± 2.5
Metaphase astral diameter (μm)	30.5 ± 5.5	55.1 ± 7	45.1 ± 7	25.0 ± 3
Aster–pole distance at anaphase onset (μm)	17.7 ± 2	15.1 ± 5	16.3 ± 3.2	27.6 ± 1.5
Aster-equator distance at anaphase onset (μm)	34.3 ± 2	28.6 ± 4.6	32.3 ± 5	39.7 ± 2
Maximum anaphase spindle length (μm)	42.5 ± 6.6	56.1 ± 4	22.4 ± 2.5	25.5 ± 2.5
Maximum anaphase chromosome segregation (μm)	52.4 ± 4.8	38.0 ± 5	31.3 ± 8.2	27.5 ± 1.5

All measurements were made on image files of either tubulin-immunofluorescent or Hoechst-stained, fixed cells using measuring tools on either Leica or MetaMorph software. Each measurement represents the mean value obtained from at least five independent measurements. ± represents range of data.

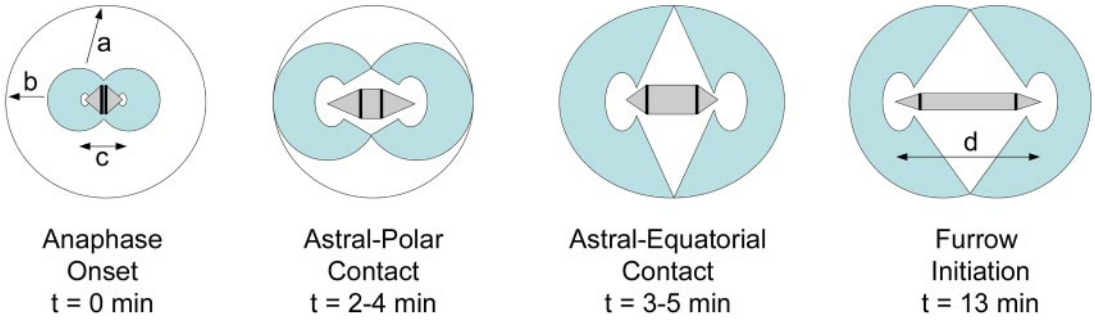

Figure 2. Geometric diagram of the MA relative to the cell cortex during anaphase. From confocal images of fixed cells stained for microtubules, we measured the distances of the polar-directed (a) and equatorially directed (b) astral MTs to the cell cortex at the time of anaphase onset, the spindle length at anaphase onset (c), and the spindle length at the time of furrow initiation (d). These measurements were used in conjunction with our analysis of anaphase astral MT growth rates to predict the time of contact between astral MTs and the polar versus equatorial cortex, relative to the time of furrow ingression.

furrow (late). We then determined the fluorescence intensity from the specified regions, calculated the average intensity of each region in each group (n = 5), and plotted the ratio of pole:equator fluorescence (Figure 3B). A value greater than 1 shows greater polar density, whereas <1 indicates a greater equatorial density.

Consistent with our observation that astral MTs directed toward the poles contact the cortex earlier than those directed toward the equator, MT density was greater at the poles than at the equator in the early cells that were fixed just after anaphase onset. However, in the middle group of cells that were fixed at the time of furrow induction, we found that the pole:equator ratio was very near 1, demonstrating that the MT density is equal at the time of furrow initiation and during the period of cleavage stimulus. Furthermore, the density of MTs at the pole versus equator remained equal in cells that had initiated cytokinesis (Figure 3). These data indicate that the density of astral MT contact with the polar versus equatorial cortex is the same at the time the stimulation of furrowing occurs, and therefore MT density alone is not a determining factor in furrow initiation. In support of this conclusion is the finding that astral MTs emanating toward the polar and the equatorial cortex become uniformly acetylated during anaphase (our unpublished data), suggesting that all populations of astral MTs become stabilized and elongate during anaphase before contacting the cell cortex.

Microtubules Undergoing Persistent Elongation Are Able to Stimulate a Cleavage Furrow

To investigate the influence of MT dynamics on furrow initiation, we treated eggs with small molecule compounds that alter MT dynamics and assessed their effects on cytokinesis. Hexylene glycol (HG) has been reported to increases MT stability (Oka *et al*., 1991; Conrad *et al*., 1994; Tirnauer *et al*., 2004). We treated metaphase eggs with HG and then added a dose of nocodazole (NZ) sufficient to depolymerize the asters in control cells (Figure 4A). Imaging of MTs revealed that pretreatment with 0.75% HG protected the asters from depolymerization by NZ, indicating that HG stabilizes astral MTs. Treatment with 0.75% HG alone resulted in a robust MA compared with controls (Figure 4B). Cells fixed shortly after HG treatment while still in metaphase had dense asters with an average diameter of 55.1 ± 3 μm, compared with 30.5 ± 5.5 μm in untreated controls (Table 1). With larger metaphase asters, the MTs at anaphase have a shorter distance to travel to the cortex to stimulate furrowing. The astral MTs directed toward the pole must grow 15.1 μm, and those directed toward the equator must grow 28.6 μm (Table 1). Similar to controls, we found that in cells fixed during early anaphase, the density of MT-cortical contact was greatest at the poles, but that in cells fixed slightly later in anaphase but before furrow ingression, astral MTs contacted the cortex at all points around the cell perimeter with equal density (Figure 4B). We found that in HG-treated cells,

Table 2. Dynamic parameters of dividing *L. pictus* eggs

Measurement	Control	HG	Taxol	Urethane
Polar anaphase astral MT growth rate (μm/min)	10 ± 2	8.2 ± 2	na*	na*
Equatorial anaphase astral MT growth rate (μm/min)	8.3 ± 2	8.0 ± 2	na*	na*
Rate of anaphase chromosome segregation (μm/min)	4.0 ± 0.5	4.0 ± 1	3.7 +/- 1	4.2 ± 0.5
Rate of furrow ingression (μm/min)	15 ± 2	12 ± 1	10 ± 5	na*
Time from anaphase onset to furrow initiation (min)	13 ± 0.5	9.5 ± 1	na*	na*

All measurements were made on time-lapse stacks of either GFP-EB1-microinjected or Hoechst-stained cells, acquired using either Leica or MetaMorph imaging software. Each measurement represents the mean value obtained from at least five independent measurements. ± represents the range of data.

*na indicates either that we were unable to make accurate measurements of the dynamic parameter being assessed or that the parameter was not relevant under the condition being tested.

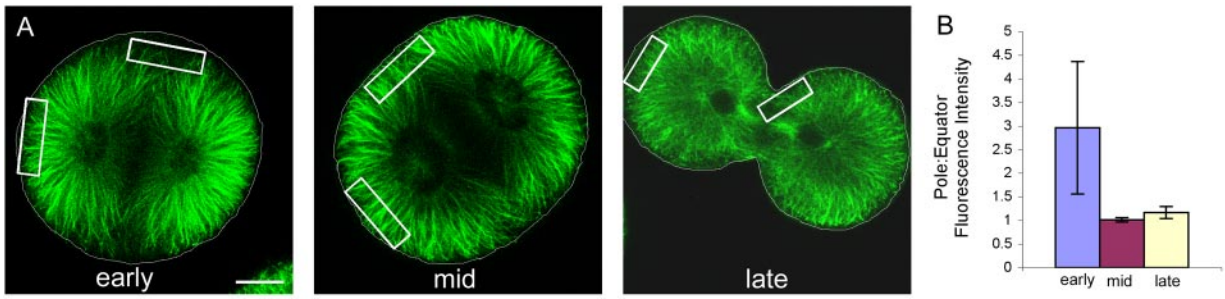

Figure 3. Microtubule density is equal in the polar versus equatorial cortex at the time of furrow initiation. Cell outlines are shown in white. (A) Confocal immunofluorescence of microtubules shortly after anaphase onset (early), just before furrow initiation (mid), and during cytokinesis (late). To estimate MT density at different locations of the cortex, polar and equatorial regions of interest were defined (white boxes), and the Leica imaging software was used to quantify the fluorescent signal from each region. Bar, 30 μm. (B) Polar and equatorial fluorescence intensities were collected from five cells in each group and then averaged. The average value of the pole:equator ratio was then plotted to reveal that MT density is greater at the poles relative to the equator in the early group of cells, but that polar and equatorial MT densities are nearly equal before initiation of the furrow, and then remain equal during ingression.

the cleavage furrow began ingression 3.5 min earlier relative to anaphase onset than in untreated controls (Table 2). Thus, astral MTs contact the cortex earlier in HG cells than in untreated controls and HG promotes MT growth either by accelerating the polymerization of MTs or by preventing MT catastrophe.

To observe the effect of HG on MT dynamics, we microinjected GFP-EB1 and then imaged the injected cells by confocal time-lapse microscopy (Figure 4C and Supplemental Movies 6 and 7). In HG-treated cells, GFP-EB1 bound along the length of the MT lattice, rather than just at the tips (Figure 4D). EB1 has been shown to associate with elongating MT tips with a higher affinity than the MT lattice but will bind along the length of stabilized MTs, such as occurs during interphase (Morrison and Askham, 2001; Tirnauer *et al*., 2002; Piehl and Cassimeris, 2003). The binding of GFP-EB1 along the MT lattice in HG-treated cells suggests stabilization of the astral MTs, therefore leading to persistent elongation during anaphase.

We tracked the growth rates of individual anaphase astral MTs growing toward the poles or equator (Figure 4E) and found that MTs in HG-treated cells grew at nearly the same

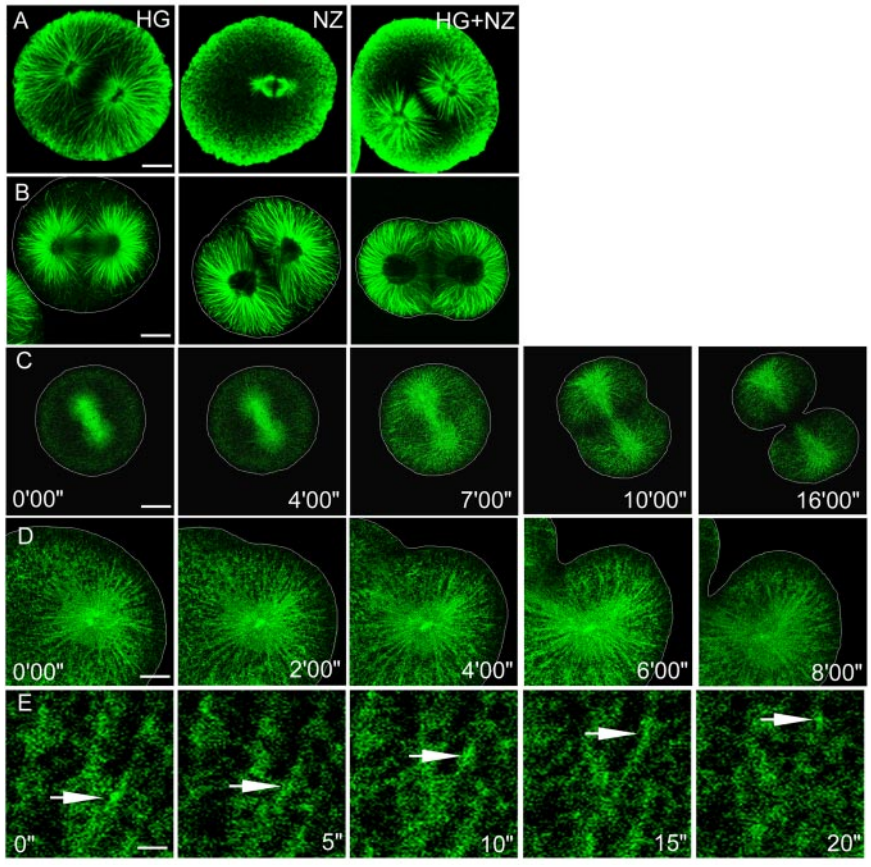

Figure 4. Hexylene glycol stabilizes microtubules and promotes precocious growth of anaphase asters. Cell outlines are shown in white when necessary. (A) Confocal immunofluorescence of microtubules in metaphase and anaphase sea urchin eggs treated with 0.75% hexylene glycol. The astral MTs seem robust and elongated relative to controls at metaphase, anaphase, and at the time of furrow ingression. Bar, 20 μm. (B) Pretreatment of eggs with 0.75% hexylene glycol protects astral microtubules from depolymerization by 1 μM nocodazole. Although 1 μM nocodazole is a sufficient dose to depolymerize the majority of the astral MTs, the addition of hexylene glycol before nocodozole permits elongation of the asters, demonstrating that hexylene glycol has a stabilizing effect on MTs. Bar, 25 μm. (C) Confocal time-lapse of a GFP-EB1-microinjected egg treated with 0.75% hexylene glycol. A robust MA, precocious anaphase astral MT elongation, and premature furrowing are apparent. Bar, 30 μm. (D) High-magnification confocal time lapse of an anaphase aster during furrow initiation in a HG-treated cell. GFP-EB1 is seen to decorate many MTs along the length of their lattice, rather than just at the tips, suggesting prolonged periods of growth and decreased catastrophe. Bar, 15 μm. (E) Confocal time lapse showing elongation of an astral microtubule during anaphase, in a cell treated with 0.75% HG. Bar, 5 μm.

rate as in untreated controls, an average of 8.2 ± 2 μm/min for polar-directed astral MTs and 8.0 ± 2 μm/min for MTs directed toward the equator (Table 2). Because HG did not seem to affect the rate of MT assembly and promoted the binding of GFP-EB1 along the MT lattice, we conclude HG promotes MT stability and elongation by reducing MT catastrophe or promoting rescue. Furthermore, HG treatment results in premature stimulation of cytokinesis coincident with early contact between the elongating asters and the cell cortex. These experiments support the idea that stabilized MTs are sufficient to stimulate a furrow.

Hexylene glycol had additional effects on the structure of the MA. We measured the length of the mitotic spindle by determining the distance between the spindle poles in confocal images of immunofluorescent cells stained for tubulin. The pole-to-pole length of the spindle at metaphase was longer in HG-treated cells, averaging 35.4 ± 4 μm, compared with 29.8 ± 3 μm in untreated controls (Table 2). During anaphase, at the time of furrow ingression, the distance between spindle poles in HG-treated cells had increased to 56.1 ± 4 μm, compared with 42.5 ± 6.6 μm in control cells (Table 1). Despite the effect of HG on spindle length, it did not affect the rate of chromosome segregation during anaphase, which was measured to be 4 μm/min in both groups (Table 2). Chromosome segregation rates were measured by time-lapse microscopy of Hoescht-stained cells. These results are consistent with HG increasing the stability of the antipolar spindle midzone MTs and thus resulting in an elongated spindle.

Microtubules with Diminished Dynamics Are Able to Stimulate a Cleavage Furrow

We next assessed the effects of taxol (paclitaxel) on the ability of the MA to stimulate cytokinesis. Taxol is an MT stabilizer that results in reduced dynamic behavior and suppression of MT disassembly (Checchi *et al*., 2003). Treatment with taxol resulted in a metaphase MA with very dense asters of a large average diameter of 45.1 ± 7 μm, relative to 30.5 ± 5.5 μm in controls (Figure 5A and Table 1). Time-lapse imaging of GFP-EB1 revealed that the asters of taxol-treated cells did not significantly expand during anaphase, and GFP-EB1 gradually became dispersed from MTs, indicating suppression of MT dynamics (Figure 5, B and C, and Supplemental Movies 8 and 9) (Yvon *et al*., 1999). Anaphase astral MTs did not undergo periods of elongation long enough for us to track, making it impossible to obtain measurements of growth rates.

The effect of taxol treatment on mitotic progression was variable. Taxol-treated cells were generally unable to undergo anaphase chromosome segregation, likely due to activation of the spindle checkpoint and subsequent metaphase arrest. Among the cells that were able to complete mitosis, chromosome segregation occurred at 3.7 ± 1 μm/min, slightly slower than in controls (Table 2). The spindle was unable to substantially elongate beyond its metaphase length of 21.8 ± 0.5 μm (Table 1), again suggesting that taxol suppressed the growth and increased stability of spindle midzone MTs whose lengthening is normally required for pole-to-pole separation. Of the taxol-treated cells that underwent anaphase chromosome movements and eventually telophase, 10 of 40 cells cleaved, forming equatorial furrows that ingressed at the plane of the former metaphase plate with the rate of furrowing significantly diminished. Of the taxol-treated cells able to undergo anaphase, 8/40 failed to initiate cytokinesis, and the remaining 22/40 displayed aberrant furrowing or cortical contractility that failed to result in cleavage.

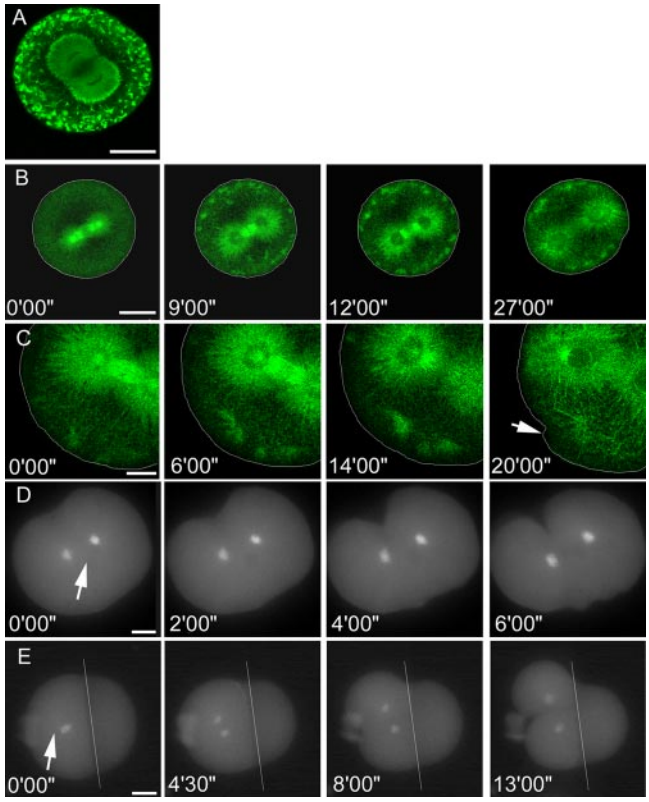

Figure 5. Taxol treatment results in diminished MT dynamics but does not prevent furrow formation. Cell outlines are shown in white when necessary. (A) Confocal immunofluorescence of microtubules in a metaphase cell treated with 100 μM taxol. The asters are extremely dense and slightly longer than the metaphase asters of control cells. The centrosomes are abnormally shaped ellipses. Many cytosolic MTs are also present. Bar, 40 μm. (B) Confocal time-lapse of a GFP-EB1-microinjected cell, treated with 50 μM taxol at metaphase. The density and length of astral MTs was increased at metaphase, but as anaphase progressed, GFP-EB1 binding diminished, suggesting suppression of dynamics. Astral MTs did not seem to substantially elongate beyond their metaphase length. The cytoplasmic clusters of MTs were observed in high abundance near the equatorial cortex. The cell elongated, but furrowing was never observed despite the fact that mitosis completed. Bar, 50 μm. (C) High-magnification confocal time-lapse of GFP-EB1 during metaphase/anaphase transition in a 50 μM taxol-treated cell. The cell did not initiate a conventional cleavage furrow, but cortical contractility occurred at sites associated with cytasters (arrow). Cell outline is shown in white. Bar, 20 μm. (D) Time-lapse of Hoechst-stained chromosomes in a cell that was microinjected with 100 μM taxol on one side of the anaphase MA (arrow indicates injection site). Microinjection blocked furrow formation on the side of injection but a normal cleavage furrow formed on the opposite side, indicating local suppression of MT dynamics on the injected side. (E) Localized microinjection of 100 μM taxol followed by micromanipulation of the MA into contact with the cortex permits initiation of a furrow. Bar, 20 μm. (White line indicates position of glass manipulator. Arrow indicates injection site.)

In a previous study, a high dose of taxol was microinjected into sea urchin eggs against one side of the anaphase MA, resulting in failure of furrowing on this side of the cell, local suppression of MT dynamics, and dense asters that failed to elongate (Hamaguchi, 1998). Consistent with Hamaguchi's results, we found that cells microinjected with taxol formed unilateral furrows in the equatorial plane on

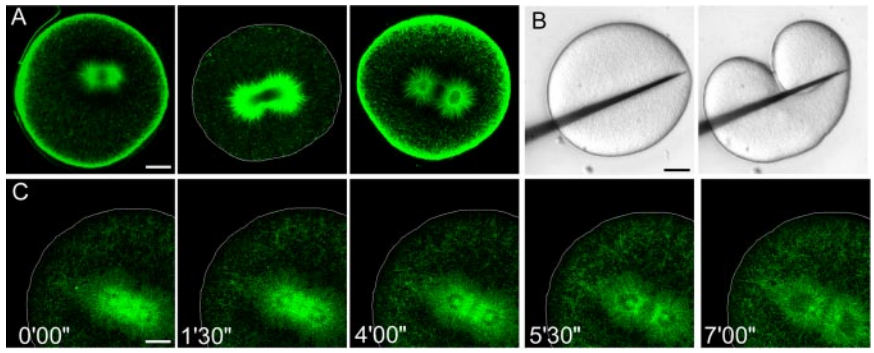

Figure 6. Urethane treatment results in short, dense asters undergoing increased catastrophe, but does not inhibit furrowing if the MA is micromanipulated toward the cortex. (A) Confocal immunofluorescence of microtubules during metaphase, anaphase, and cytokinesis in cells treated with 60 mM urethane. The asters are reduced in size and never elongate during anaphase. They do seem to become more dense during anaphase, consistent with increased occurrence of catastrophe, followed by brief periods of elongation. The spindle is reduced in length relative to controls, and never elongates before telophase, suggesting an absence of anaphase b. Bar, 20 μm. (B) Nomarski DIC image showing that micromanipulation of the MA toward the cortex in a urethane treated cell results in furrowing. Bar, 20 μm. (C) Confocal time lapse of a GFP-EB1-microinjected cell, treated with 60 mM urethane at metaphase. The asters are diminished in length but highly dynamic. The centrosomes do not substantially expand and the spindle poles do not separate during anaphase. Bar, 15 μm.

the uninjected side of the MA and failed to furrow on the injected side (Figure 5D and Supplemental Movie 10). Hamaguchi concluded that taxol-stabilized MTs were unable to stimulate a furrow. We wished to determine whether the failure to furrow on the injected side was the result of altered MT dynamics, or the failure of the astral MTs to contact the cortex. To distinguish between these two possibilities, we microinjected 100 μM taxol on one side of the MA at anaphase onset and then used a glass microneedle to manipulate the taxol-injected side of the MA against the cortex (Figure 5E and Supplemental Movie 11). In three independent experiments, a furrow formed at the normal equatorial site on the taxol-injected side of the cell, after micromanipulation. These experiments suggest that stabilized MTs are sufficient to stimulate a furrow.

Microtubules Undergoing Increased Catastrophe Are Able to Stimulate a Cleavage Furrow

Urethane (ethyl carbamate) is a small molecule compound that has been used as an MT inhibitor (Rappaport and Rappaport, 1984; Rappaport, 1996). Eggs that are treated with urethane undergo mitosis, but they become binucleate due to failure to initiate cytokinesis (Figure 6A). Visualization of MTs by immunofluorescence in mitotic sea urchin eggs treated with 60 mM urethane revealed that astral MTs were diminished in length, with an average astral diameter of 25 μm at metaphase (Table 1). During anaphase, the asters became dense with MTs, but they failed to elongate and did not contact the cortex. The metaphase pole-to-pole spindle distance also was reduced in length relative to controls, at 19.7 $\pm$ 2.5 μm compared with 29.8 $\pm$ 3 μm for controls, and they remained short throughout mitosis, elongating to an average of just 25.5 $\pm$ 2.5 μm (Figure 6 and Table 1).

Rappaport showed previously that micromanipulation of the MA toward the cortex in a urethane-treated cell results in initiation of a furrow (Rappaport and Rappaport, 1984). We were able to confirm this finding (Figure 6B) and were therefore interested in the dynamic state of MTs in cells that have been treated with urethane. The reduced length of the MTs in urethane-treated cells could be due either to increased catastrophe or decreased polymerization. To distinguish between these possibilities and assess the effects of urethane on MT dynamics, we microinjected GFP-EB1into fertilized eggs and imaged them by confocal time-lapse microscopy (Figure 6C and Supplemental Movie 11). MT polymerization did not seem to be affected by urethane treatment, because GFP-EB1 decorated the tips of elongating MTs in all portions of the MA with an equal intensity of brightness to that seen in untreated controls, and elongated for brief periods with a velocity resembling that of controls. Typical EB1 comet tails were seen to emanate from the centrosomes at both poles, revealing rapid phases of astral MT elongation; however, the asters failed to expand during anaphase beyond their metaphase diameter. Furthermore, the asters increased in density at anaphase onset, indicating increased polymerization, which is a normal event associated with the metaphase-anaphase transition. It therefore seems that the shortened MTs in urethane-treated cells result from increased catastrophe, rather than slowed elongation. Our criteria for measuring MT growth rates were that the MT tip must remain in the confocal plane through three acquisitions at 5-s intervals. In urethane-treated cells, we were unable to identify any MTs that met these criteria, arguing that the MTs underwent very short periods of elongation before catastrophe. These findings indicate that urethane suppresses MT growth by increasing MT catastrophe and not by decreasing polymerization. The fact that urethane-treated cells initiated a furrow upon manipulation of the MA to the cortex demonstrates that MTs with increased catastrophe are sufficient to stimulate a furrow. We conclude that stable MTs are not required for initiation of cytokinesis.

DISCUSSION

Microtubules of the MA are required for stimulation of cytokinesis; however, the nature of this requirement is unknown. In the large spherical eggs of echinoderms, the astral microtubules are responsible for communication of signals to the cortex (Rappaport, 1996). We find that cytokinesis can be stimulated under conditions that suppress MT dynamics, promote MT elongation, or promote MT catastrophe, as long as MT plus ends are able to physically contact the cell cortex.

Stable MTs Are Not Required for Furrow Initiation

It has been reported that MT stabilization correlates with stimulation of cytokinesis because furrowing occurred at sites of contact between chromosome associated stable MTs and the cortex in tissue culture cells and that selective stabilization of equatorially directed astral MTs occurs as a result of their elongation past the chromosomes during anaphase (Canman *et al*., 2003). Astral MTs that contacted the cortex but then retracted due to dynamic instability were not observed to correlate with furrow ingression (Canman *et al*., 2003). This report that furrow formation corresponds to sites

of stable MT contact is consistent with the finding that flattened sea urchin eggs treated with taxol and containing multiple MAs formed furrows when the MAs were near the surface (Salmon and Wolniak, 1984). These studies show that stable MTs are sufficient for furrow induction but do not address the question of whether the stabilized state of the astral MTs specifically contributes to furrow initiation or whether stabilization only facilitates persistent contact with the cortex.

In the cells that we studied in this report, the astral MTs that stimulate a furrow, are not associated with chromosomes; therefore, some other aspect of the astral MTs must be responsible for induction of the furrow. We directly tested the role of MT stability in furrow initiation by using small molecule drugs to modulate MT dynamics. We hypothesized that if stable astral MT contact with the cortex is required for stimulation of cytokinesis, then highly unstable astral MTs would not be able to stimulate a furrow, even under circumstances of physically induced contact with the cortex. We analyzed the ability of the anaphase astral MTs to stimulate furrowing in a variety of dynamic backgrounds and found that the dynamic state of the MTs was dispensable for furrow initiation but that persistent contact with the cortex was required in all cases.

The artificially stabilized MTs of cells treated with HG displayed persistent elongation, which resulted in early contact between astral MTs and the cortex, and premature furrow formation (Figure 4 and Table 1). This is consistent with our previous findings showing that precocious furrowing could be induced by bringing the cell cortex into proximity to the MA after anaphase onset (Shuster and Burgess, 1999, 2002). Suppression of MT dynamics with taxol produced dense asters that failed to elongate at anaphase. Observations of MTs in taxol-treated cells microinjected with GFP-EB1 revealed that furrows formed only in cases where contacts between the MA and the cell cortex were established (Figure 5 and Supplemental Movie 9). Microinjection of a high concentration of taxol against one side of the anaphase MA, which has been shown to prevent local MT growth (Hamaguchi, 1998) did not inhibit furrowing when the taxol side of the MA was manipulated into contact with the cortex (Figure 5). Our results are therefore consistent with previous observations that taxol-treated eggs with multiple MAs were able to form furrows if the MA was in proximity to the cell surface (Salmon and Wolniak, 1984). Therefore, suppression of MT dynamics does not disrupt their ability to stimulate cytokinesis.

Treatment with the MT inhibitor urethane produced short, dense anaphase asters and a small spindle, which undergoes very little anaphase B, due to increased MT catastrophe and brief periods of MT growth (Figure 6 and Supplemental Movie 12). The urethane-treated MA also was competent to stimulate furrowing if manipulated into contact with the cortex, demonstrating that MT stability is not required for initiation of cytokinesis (Figure 6). Our interpretation of these findings is that the cell cortex is insensitive to the dynamic state of microtubules during anaphase.

Contact between Astral MTs and the Cell Cortex Occurs Earlier than Furrow Initiation

Rappaport's work on dividing echinoderm eggs indicates that the contractile signal emanates from the asters at a rate of 6–7 μm/min, remarkably close to our observed growth rate of astral MTs, and that the signal must interact with the cortex for 1 min followed by a 3-min lag period before furrow initiation (Rappaport and Ebstein, 1965; Rappoport, 1973). Our data indicate that MTs grow at ~9 μm/min, and that furrowing begins ~13 min after anaphase onset (Tables 1 and 2). During this 13 min, we find that the MTs growing toward the equator (the site of furrowing) traverse a distance of ~35 μm and sustain 7–10 min of interaction with the cortex before furrowing onset, whereas those directed toward the poles travel half the distance and sustain even longer periods of cortical interaction, suggesting that contact alone is not sufficient to induce furrowing (Tables 1 and 2). Our determination of astral MT–equatorial cortical contact time in normal spherical cells is more than twice the 4-min stimulatory and delay period required by Rappaport's experiments and thus suggests that MT contact alone is not the determining factor in signaling cytokinesis in eggs.

One possibility is that astral MTs become stabilized by their interaction with the cortex once contact has been made. If such a mechanism were spatially reinforced such that equatorially directed astral MTs were selectively stabilized upon contact with the cortex, then these stable MTs could serve as persistent tracks for signal delivery, directly to the site of contractile ring assembly. Although such a mechanism has yet to be elucidated, the time-lapse images of GFP-EB1 in dividing cells reported here reveal that GFP-EB1 on equatorially-directed MT tips is diminished during furrow initiation, relative to polar-directed MT tips (Figure 1C). Immunofluorescence of tubulin reveals that many astral MTs oriented toward the equator exist at the time of furrow initiation (Figure 1A). The fact that fewer EB1 comet tails emanate toward the equatorial sites suggests that these MTs may be preferentially stabilized, whereas the polar-directed astral MTs may remain dynamic, undergoing continuous rounds of growth and catastrophe in the absence of a stabilizing cortical interaction in the polar region.

Our analysis of individual MTs using GFP-EB1 to track growing MT ends demonstrates that polar and equatorial astral MTs elongate at comparable rates during anaphase (Table 2); however, polar MTs have a shorter distance to the cortex and make first contact. These data could therefore support the "polar relaxation" hypothesis of furrow initiation in normal spherical cells, which suggests that astral MTs have a relaxing influence on the contractility of the cortex and prevent furrow formation at their sites of polar cortical contact by relieving tension. However, polar relaxation, if strictly due to MT contact, requires a local minimum of MT density at the equator during the time of the stimulus. Different MT densities between the pole and the equatorial cortex have been observed in sea urchin eggs and in *C. elegans* embryos although these studies were unclear as to whether microtubule density was determined at the time of the cleavage stimulus (Asnes and Schroeder, 1979; Dechant and Glotzer, 2003). Our findings represent the first demonstration that MT density is equal throughout the cortex during the period of cleavage stimulus. Although the equatorial MT density minimum required by the polar relaxation model exists early during early anaphase, our results indicate that this condition does not exist at the time of furrow stimulation (Figures 2 and 3).

Questions of how astral MTs promote differentiation between the polar and equatorial environments remain to be addressed. Our findings argue that astral MTs convey their contractile stimulus to the cortex via some property other than their dynamics or density. Originally, it was hypothesized that a maximum concentration of contractile signals arises as the equator because this site receives stimulation from both asters. However, the fact that monopolar spindles are able to induce furrowing in tissue culture cells (Canman *et al*., 2003), and in eggs (Rappaport, 1991), and at the poles of bipolar MAs in eggs (Rappaport, 1991) are able to induce

a furrow, refutes this idea. One possible explanation is that the tips of the astral MTs convey spatial and temporal information to the cortex as they elongate at anaphase. Several MT plus end binding proteins have emerged as intriguing candidates for mediators of this communication between the MA and the cortex. These proteins, including EB1, $p150^{glued}$, APC, CLIP-170, and others have been shown to affect MT dynamics and may therefore be involved in promoting MT growth toward the cortex at anaphase onset and differentiation between equatorial versus polar astral MTs (Akhmanova and Hoogenraad, 2005). They also may play additional downstream roles in furrow initiation, because many of these proteins form complexes with one another, leading to the proposal of a MT plus end "raft." Such complexes may facilitate search and capture events between growing MTs and their intracellular targets, such as kinetochores or the cell cortex (Mimori-Kiyosue *et al*., 2000; Tirnauer and Bierer, 2000; Gundersen, 2002; Carvalho *et al*., 2003; Galjart and Perez, 2003; Gundersen *et al*., 2004; Vaughan, 2004). Localization of MT plus end binding proteins to the cell cortex could provide cortical receptor sites for elongating MTs. Indeed, such an interaction has been shown to promote nuclear positioning during cell division in yeast (Lee *et al*., 2000). Alternatively, concentration of an MT binding cortical receptor to a specific region could allow anaphase astral MTs to establish stable lines of communication in a targeted manner.

In the experiments presented here, we have shown that stable MTs are not required for furrow ingression as long as MA MTs are manipulated into contact with the cortex. It is possible that micromanipulation of the MA eliminates the need for stable contact by forcing all of the factors associated with the MA against the cortex. This study therefore does not exclude the possibility that in nonmanipulated cells, some sort of stabilizing interaction between the asters and the cortex is necessary to allow for delivery of the contractile stimulus over such a substantial distance. Indeed, classic experiments in which blocking contact between the equatorial cortex and the MA was shown to compromise cytokinesis (Rappaport, 1969) may argue in favor of stable contact. Our interpretation of these studies is that although prolonged contact seems to be necessary, the astral MTs inducing the furrow need not be stable because micromanipulation of urethane-treated asters toward the cortex achieves prolonged contact between destabilized population of astral MTs and the cell cortex, and results in furrow formation.

Our findings that astral MT contact with the cortex is required for furrow initiation, and that this contact must occur after anaphase onset (Shuster and Burgess, 2002), reinforce the idea that the metaphase–anaphase transition results in a biochemical environment that is supportive of cytokinesis but that furrow ingression requires the partitioning of cytoplasm that is accomplished by MTs as they elongate during anaphase.

ACKNOWLEDGMENTS

We are grateful to Lynne Cassimeris for providing the hEB1 construct that was used by Michelle Ng to produce the hEB1-EGFP fusion protein used in these studies and to Brad Shuster for providing wide field immunofluorescence images of tubulin in dividing sea urchin eggs as well as for advice during preparation of this manuscript. We also acknowledge Gregg Gundersen for advice on the manuscript. Funding was provided by the National Institutes of Health Grant GM-58231.

REFERENCES

Akhmanova, A., and Hoogenraad, C. C. (2005). Microtubule plus-end-tracking proteins: mechanisms and functions. Curr. Opin. Cell Biol. *17*, 47–54.

Asnes, C., and Schroeder, T. E. (1979). Cell cleavage. Ultrastructural evidence against equatorial stimulation by aster microtubules. Exp. Cell Res. *122*, 327–338.

Balasubramanian, M., Bi, E., and Glotzer, M. (2004). Comparative analysis of cytokinesis in budding yeast, fission yeast, and animal cells. Curr. Biol. *14*, R806–R818.

Beams, W. H., and Evans, T. C. (1940). Some effects of colchicine upon the first cleavage in *Arbacia punctualta*. Biol. Bull. *79*, 188–198.

Burgess, D. R., and Chang, F. (2005). Site selection for the cleavage furrow at cytokinesis. Trends Cell Biol. *15*, 156–162.

Canman, J., Cameron, L., Maddox, P., Straight, A., Tirnauer, J., Mitchison, T., Fang, G., Kapoor, T., and Salmon, E. (2003). Determining the position of the cell division plane. Nature *424*, 1074–1078.

Carvalho, P., Tirnauer, J. S., and Pellman, D. (2003). Surfing on microtubule ends. Trends Cell Biol. *13*, 229–237.

Checchi, P. M., Nettles, J. H., Zhou, J., Snyder, J. P., and Joshi, H. C. (2003). Microtubule-interacting drugs for cancer treatment. Trends Pharmacol. Sci. *24*, 361–365.

Conrad, A. H., Stephens, A. P., and Conrad, G. W. (1994). Effect of hexylene glycol-altered microtubule distributions on cytokinesis and polar lobe formation in fertilized eggs of *Ilyanassa obsoleta*. J. Exp. Zool. *269*, 188–204.

D'Avino, P. P., Savoian, M. S., and Glover, D. M. (2005). Cleavage furrow formation and ingression during animal cytokinesis: a microtubule legacy. J. Cell Sci. *118*, 1549–1558.

DeBrabander, M., Geuens, G., Nuydens, R., Willebrords, R., Aerets, F., and DeMay, J. (1986). Microtubule dynamics during the cell cycle: the effects of taxol and nocodazole on the microtubule system of PtK2 cells at different stages of the mitotic cycle. Int. Rev. Cytol. *101*, 215–274.

Dechant, R., and Glotzer, M. (2003). Centrosome separation and central spindle assembly act in redundant pathways that regulate microtubule density and trigger cleavage furrow formation. Dev. Cell *3*, 333–344.

Galjart, N., and Perez, F. (2003). A plus-end raft to control microtubule dynamics and function. Curr. Opin. Cell Biol. *15*, 48–53.

Glotzer, M. (2005). The molecular requirements for cytokinesis. Science *307*, 1735–1739.

Gundersen, G. (2002). Microtubule Capture: IQGAP and CLIP-170 Expand the Repertoire. Curr. Biol. *12*, 645–647.

Gundersen, G. G., Gomes, E. R., and Wen, Y. (2004). Cortical control of microtubule stability and polarization. Cur. Opin. Cell Biol. *16*, 106–112.

Hamaguchi, Y. (1998). Displacement of cleavage plane in the sea urchin egg by locally applied taxol. Cell Motil. Cytoskeleton *40*, 211–219.

Lee, L., Tirnauer, J. S., Schuyler, S. C., Liu, J. Y., and Pellman, D. (2000). Positioning of the mitotic spindle by a cortical-microtubule capture mechanism. Science *287*, 2260–2262.

Mallavarapu, A., Sawin, K., and Mitchison, T. J. (1999). A switch in microtubule dynamics at the onset of anaphase B in the mitotic spindle of *Schizosaccharomyces pombe*. Curr. Biol. *9*, 1423–1426.

Mimori-Kiyosue, Y., Shiina, N., and Tsukita, S. (2000). The dynamic behaviour of the APC-binding protein EB1 on the distal ends of microtubules. Curr. Biol. *10*, 865–868.

Morrison, E. E., and Askham, J. M. (2001). EB 1 immunofluorescence reveals an increase in growing astral microtubule length and number during anaphase in NRK-52E cells. Eur. J. Cell Biol. *80*, 749–753.

Oka, M. T., Arai, T., and Hamaguchi, Y. (1991). Change in the heterogeneous distribution of tubulin isotypes in mitotic microtubules of the sea urchin egg by treatment with microtubule depolymerizing or stabilizing drugs. Cell Struct. Funct. *16*, 125–134.

Piehl, M., and Cassimeris, L. (2003). Organization and dynamics of growing microtubule plus ends during early mitosis. Mol. Biol. Cell *14*, 916–925.

Piehl, M., Tulu, U. S., Wadsworth, P., and Cassimeris, L. (2004). Centrosome maturation: measurement of microtubule nucleation throughout the cell cycle using GFP-tagged EB1. Proc. Natl. Acad. Sci. USA *101*, 1584–1588.

Rappaport, R. (1969). Aster-equatorial surface relations and furrow establishment. J. Exp. Zool *171*, 59–68.

Rappaport, R. (1973). On the rate of movement of the cleavage stimulus in sand dollar eggs. J. Exp. Zool. *183*, 115–119.

Rappaport, R. (1991). Enhancement of aster-induced furrowing activity by a factor associated with the nucleus. J. Exp. Zool. *257*, 87–95.

Rappaport, R. (1996). Cytokinesis in Animal Cells, Cambridge: Cambridge University Press.

Rappaport, R., and Ebstein, R. P. (1965). Duration of stimulus and latent periods preceding furrow formation in sand dollar eggs. J. Exp. Zool. *158*, 373–382.

Rappaport, R., and Rappaport, B. N. (1984). Division of constricted and urethane-treated sand dollar eggs: a test of the polar stimulation hypothesis. J. Exp. Zool. *231*, 81–92.

Rusan, N. M., Tulu, U. S., Fagerstrom, C., and Wadsworth, P. (2002). Reorganization of the microtubule array in prophase/prometaphase requires cytoplasmic dynein-dependent microtubule transport. J. Cell Biol. *158*, 997–1003.

Salmon, E. D., and Wolniak, S. M. (1984). Taxol stabilization of mitotic spindle microtubules: analysis using calcium-induced depolymerization. Cell Motil. *4*, 155–167.

Shuster, C. B., and Burgess, D. R. (1999). Parameters that specify the timing of cytokinesis. J. Cell Biol. *146*, 981–992.

Shuster, C. B., and Burgess, D. R. (2002). Transitions regulating the timing of cytokinesis in embryonic cells. Curr. Biol. *12*, 854–858.

Snyder, J. A., and Mullins, J. M. (1993). Analysis of spindle microtubule organization in untreated and taxol-treated PtK1 cells. Cell Biol. Int. *17*, 1075–1084.

Strickland, L., von Dassow, G., Ellenberg, J., Foe, V., Lenart, P., and Burgess, D. (2004). Light microscopy of echinoderm embryos. Methods Cell Biol. *74*, 371–409.

Tirnauer, J. S., and Bierer, B. E. (2000). EB1 proteins regulate microtubule dynamics, cell polarity, and chromosome stability. J. Cell Biol. *149*, 761–766.

Tirnauer, J. S., Grego, S., Salmon, E. D., and Mitchison, T. J. (2002). EB1-microtubule interactions in *Xenopus* extracts: role of EB1 in microtubule stabilization and mechanisms of targeting to microtubules. Mol. Biol. Cell *13*, 3614–3626.

Tirnauer, J. S., Salmon, E. D., and Mitchison, T. J. (2004). Microtubule plus-end dynamics in *Xenopus* egg extract spindles. Mol. Biol. Cell *15*, 1776–1784.

Vaughan, K. (2004). Surfing, regulating and capturing: are all microtubule-tip-tracking proteins created equal? Trends Cell Biol. *14*, 491–496.

White, J. G., and Borisy, G. G. (1983). On the mechanisms of cytokinesis in animal cells. J. Theor. Biol. *101*, 289–316.

Wilson, E. B. (1928). The Cell in Development and Heredity, 3rd ed., New York: The Macmillan Company.

Wolpert, L. (1960). The mechanics and mechanism of cleavage. Int. Rev. Cytol. *10*, 163–216.

Yvon, A. M., Wadsworth, P., and Jordan, M. A. (1999). Taxol suppresses dynamics of individual microtubules in living human tumor cells. Mol. Biol. Cell *10*, 947–959.

Zhai, Y., Kronebusch, P. J., and Borisy, G. G. (1995). Kinetochore microtubule dynamics and the metaphase-anaphase transition. J. Cell Biol. *131*, 721–734. sents the mean value obtained from at least five independent measurements. ± represents the range of data.